ELSEVIER

Contents lists available at ScienceDirect

Sensors and Actuators: B. Chemical

journal homepage: www.elsevier.com/locate/snb





Photonic microresonator based sensor for selective nitrate ion detection

Zhongbo Zhang ^{a,*}, Xufeng Zhang ^b, Tijana Rajh ^b, Supratik Guha ^a

- ^a Pritzker School of Molecular Engineering, the University of Chicago, Chicago, IL, 60637, United States
- ^b Center for Nanoscale Materials, Argonne National Laboratory, Argonne, IL, 60439, United States

ARTICLE INFO

Keywords:
Nitrate sensor
Micro-ring resonator
Ion selective membrane
Integrated photonic sensor

ABSTRACT

Sensing nitrate concentrations in soil with high sensitivity and selectivity using field-deployable compact sensor platforms is a sought-after goal for environment and agriculture applications. This study demonstrates a new optically based nitrate sensing platform based on ion-selective membrane (ISM) functionalized chip-scale photonic micro-ring resonators. Our approach relies upon measurements of resonance shifts in the micro-resonators and leverages the excellent, though little studied, optical properties of ISMs. Using a high-quality micro-ring resonator, a nitrate ion-selective photonic sensor exhibits a detection limit down to 0.1 parts per million (ppm) and enables nitrate concentration measurements in the $1-100\,\mathrm{ppm}$ level, appropriate for soil science and agriculture. Importantly, the sensor also shows high selectivity over other competing anions in soil, such as Cl^- and NO_2^- . We argue that this chip-scale approach can be incorporated into compact sensor platforms.

1. Introduction

Highly selective chemical sensing of the nitrate ion at trace levels is an important research topic for a broad range of areas from environmental sensing and soil science, to agriculture and homeland security. Nitrate is a key mineral nutrient for most plants, and its application via fertilizers is a major source of water pollution globally due to fertilizer runoff in rivers and streams [1,2]. Precision nitrogen-management and efficient fertilization can reduce the negative impact to the environment, and is desirable in modern agriculture [3]. High resolution measurements of soil nitrate concentration (10-100 ppm) is the relevant range) is also key to a better understanding of the biogeochemistry of soils and its impact on plant growth. However, a reliable field-deployed sensor technology for effectively detecting the concentration of such ions at high sensitivity, specificity and accuracy is still lacking. In-situ, compact sensing approaches relevant to nitrate detection can be categorized into two types: potentiometric methods and optical methods. For potentiometric approaches such as the ion-selective electrode (ISE) [4-6] and the ion-selective field-effect transistor (ISFET) [7,8], the intrinsic potential drift from a reference electrode cannot be avoided and the need for frequent calibration can hinder their practical applications, especially for soil sensing [9]. In contrast, optical sensing approaches for detecting nitrates have minimal electrical interference and baseline variation can be eliminated [10]. Spectrophotometric methods are well studied for nitrate/nitrite determination, including UV-vis [11,12], fluorimetric

[13,14], and chemiluminescence [15]. However, these techniques need complicated sample pretreatment, such as assay protocols involving redox reactions, which are unfavorable for field-deployed nitrate determination [10]. Other optical methods such as Fourier-transform infrared spectroscopy (FT-IR) [16,17] and Raman spectroscopy [18] for detecting nitrate have also been evaluated. Although these methods can provide outstanding sensitivity, the need for sophisticated and expensive instruments reduces the interest in these techniques beyond the laboratory.

Compared with other optical methods, silicon-based integrated photonic sensors are well known for their advantages of compact size and multiplexed sensing capability [19,20]. Our research targets at the development of small, low-cost, high-sensitivity micro-ring resonator-based photonic sensor platforms fabricated on silicon (Fig. 1a) capable of sensing ionic species such as nitrates. Such evanescently coupled resonator structures enable the detection (using refractometry measurements) of small shifts ($\sim 10^{-3}$ – 10^{-4}) in refractive indices near the resonator surface. Our strategy is to functionalize this embedding media with materials that can selectively bind to the target analyte, assuring high specificity in the sensing process. The selective binding results in a change in the refractive index which is picked up by shifts in the light absorption peak through the resonator device. In this paper, we demonstrate the feasibility of this technique for nitrate sensing. Using nanofabricated micro-ring resonators integrated with nitrate selective polymer films that undergo small but detectable changes in the

E-mail address: zxz202@uchicago.edu (Z. Zhang).

^{*} Corresponding author.

refractive index upon absorbing nitrate ions, we show that nitrate concentrations in the relevant range of $10-100\,\mathrm{ppm}$ can be detected with good specificity against Cl- and NO_2 -. These targets appropriately meet the needs for nitrate sensors geared towards soil and plant science.

The polymer films used for functionalization are ion-selective membranes (ISMs). While nitrate ISMs were exploited in techniques that monitor electrical signals [21,22], such as potentiometric thick film sensors [23,24] and ion-selective field-effect transistors (ISFETs) [7,8], ISMs are also excellent optical materials and their optical properties have not been well explored thus far. ISMs can be prepared from a polyvinyl chloride (PVC)-based polymer matrix, which is typically transparent in the visible light regime and can be integrated as optical coatings. Research on the optical properties of ISMs has been limited [25], and, while there have been some applications using ISMs in optical sensors [26], ISMs have not been adopted in highly sensitive photonic microresonators that rely on their optical refractive index response [27].

2. Results and discussion

2.1. Optical properties of ISM

The nitrate ion-selective membrane used in this work is composed of tridodecylmethylammonium nitrate (TDDMA) dispersed in an overplasticized PVC polymer matrix. The ionophore TDDMA serves as a selective ion carrier which allows only nitrate ions to enter the hydrophobic membrane from the aqueous solution (Fig. 1b). This nitrate ionophore has been widely used for preparing nitrate ion-selective membranes and has been proven to have excellent selectivity for nitrate ions when adopted in ISE and ISFET applications [28,29]. The membrane is prepared from the premixed cocktail solutions (nitrate ionophore-cocktail A, product of Sigma-Aldrich, product 72549) containing TDDMA, plasticizer, additives, and PVC that are all dissolved in tetrahydrofuran (THF) solvent.

To demonstrate the feasibility of using TDDMA ISM as the functionalization layer for a photonic sensor, the optical properties of 100- μm -thick membranes were first studied. The samples were soaked overnight in either a de-ionized (DI) water solution (as a control sample), or a solution of sodium nitrate (with a nitrate concentration of 1000 ppm), respectively. From the UV–vis measurements of optical absorption (Fig. 1c), it is clearly observed that the ISMs show low absorption in the visible light regime. The absorption coefficient of the ISM changes abruptly around $\sim\!420\,\mathrm{nm}$ in all three cases. We believe this is due to the optical absorption characteristics of the PVC polymer matrix.

For the control sample soaked in DI water, the absorption increases slightly after the soaking. For the sample soaked in the nitrate solution, the membrane absorption is reduced by a factor of three after the soaking. When the ISM is used as a functionalization coating on highly sensitive photonic devices, such a slight absorption change can be captured with high precision. According to the Kramers-Kronig relation, such a change in absorption over a broad spectral range will also result in a change in the ISM's refractive index. The refractive index change can be read out using refractometric measurement, which maybe more reliable than the absorption-based sensing techniques as it relies on spectral information that is less susceptible to external interferences. Therefore, this ISM is intrinsically a good candidate as a functionalization coating for integrated photonic sensors that can measure small changes in the refractive index. Combined with the high sensitivity of photonic sensing platforms, and using nitrate detection as an example, we show in this work that trace-level detection of ions can be achieved.

2.2. Device fabrication, simulation, and characterization

The device fabrication flow is described in Fig. 2a. Numerical simulations (Finite-Difference Time-Domain method using the Lumerical software package) of our micro-resonator device shows that the squareshaped waveguide cross-section supports one fundamental transverse electric (TE) and one transverse magnetic (TM) mode [30]. A race-track-type ring resonator is used where the micro-ring resonator and the waveguide are aligned in parallel along a length of 200 μm to ensure good coupling between the micro-ring resonator and the waveguide. A bending radius of 30 μm was used in order to achieve a balance between low optical loss (small bend radius results in high optical loss), and a large free spectral range (FSR, i.e., spectral separation of two neighboring resonances) which reduces as the bend radius increases. Ideally, the FSR should be significantly larger than the resonance shift due to the analyte detection. An optimal gap between the micro-ring and the waveguide of around 350 nm was chosen by comparing and selecting the highest extinction ratios from a set of devices with gaps varying from $\sim 100 - 600 \, \text{nm}$.

Transmission measurements are carried out by sending light from a tunable external-cavity laser through the device and monitoring the output light spectrum while the input light wavelength is scanned. A typical measured transmission spectrum of a micro-resonator is shown in Fig. 3a. A series of optical resonance dips are observed in the transmission spectrum at the wavelengths that satisfy the resonance condition $\lambda = n_{\rm eff} \times L/m$, where λ is the resonance wavelength, $n_{\rm eff}$ is the

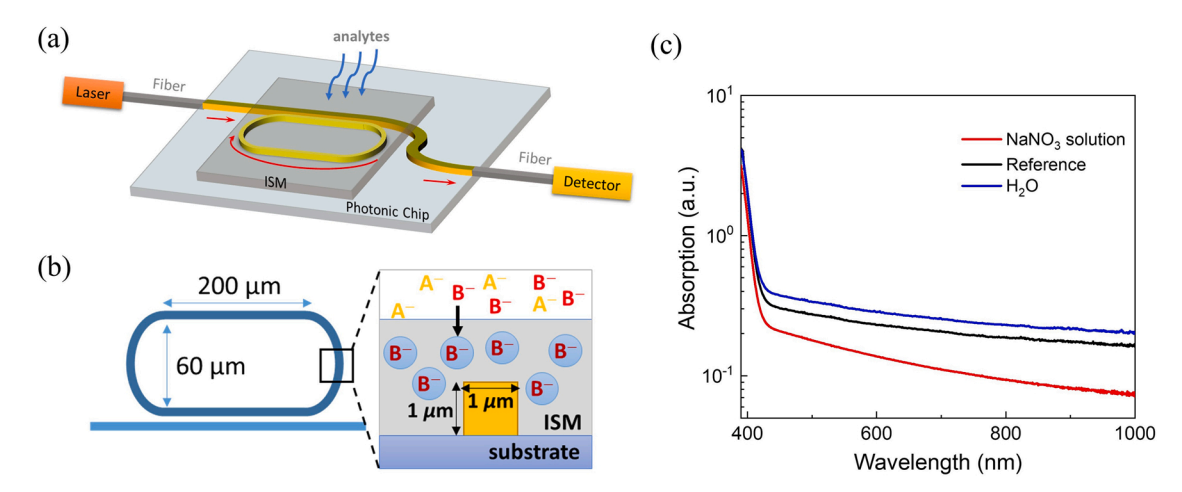


Fig. 1. (a) Schematics of the nitrate ion-selective photonic sensor. (b) Cross-sectional view of the device. ISM coating covers the micro-ring resonator and isolate the photonic device from the solution environment. The presence of the ionophore ensures only the target ions can be bond and diffuse within the membranes and affect the optical response. (c) UV–vis transmission spectrum of a 100-μm-thick nitrate ISM with different soaking conditions: no soaking (black line), soaked in water overnight (blue line), and soaked in sodium nitrate solution overnight with a concentration of 1000 ppm (red line) (For interpretation of the references to colour in this figure legend, the reader is referred to the web version of this article).

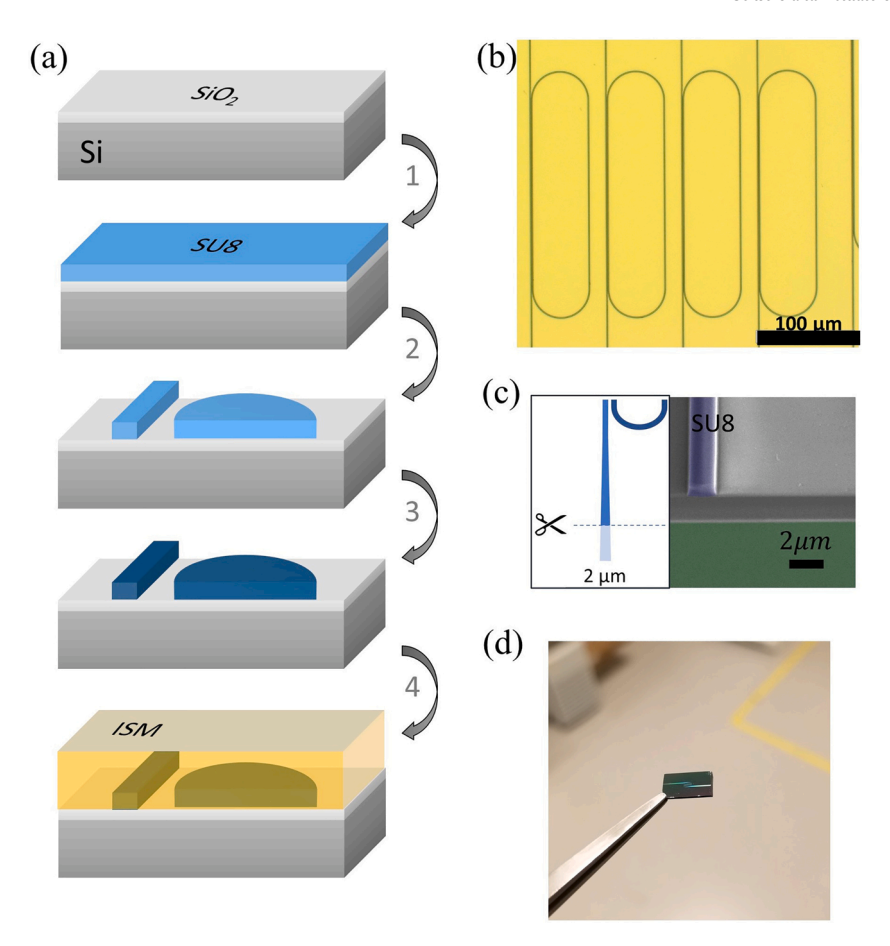


Fig. 2. (a) Device fabrication procedure. Step 1: spin coating of SU8; Step 2: electro-beam lithography and developing; Step 3: hard baking for SU8 curing; Step 4: application of the ISM to the chip surface; (b) Optical image of the fabricated SU8 micro-ring resonator; (c) Scanning electron microscopy (SEM) image of the SU8 waveguide cross-section and schematic for the tapered waveguide; (d) Image of a photonic sensor chip.

effective index of the waveguide mode, L is the total length of the microring and m is an integer mode index. The micro-resonator has a total length of $526\,\mu m$, corresponding to a FSR of $0.60\,n m$. The coupling gap between the micro-resonator to the waveguide is optimized to obtain a large extinction ratio. Because of the square shape of the waveguide cross-section, the two modes, TE and TM, are almost degenerate and their FSRs are very similar. According to $\lambda = n_{\rm eff} \times L/m$, the sensitivity can be calculated as $d\lambda/dn \approx d\lambda/dn_{\text{eff}} = \lambda/n_{\text{eff}}$, assuming n_{eff} is the refractive index of SU8 (1.564). The estimated sensitivity of such microresonators is 500 nm/RIU (RIU: refractive index unit). Without the ISM coating, the microresonator transmission spectrum shows a series of narrow resonance dips (Fig. 3a) with a linewidth ~8 pm which corresponds to a loaded Q-factor of 96,000 as shown in Fig. 3b, which is a zoomed in section from Fig. 3a. The deep, nearly symmetric curve can be well fitted by a Lorentzian function, indicating a high sensitivity and a large ratio of resonance signal/background noise. Due to the high spectral resolution of the tunable laser, sub-pm shifts in the optical resonance can be resolved, which corresponds to an approximate change of 10⁻⁴ in refractive index according to the equation $\lambda = n_{\text{eff}} \times L/m$.

The application of the ISM to the photonic chip surface alters the local refractive index near the micro-ring resonator and therefore affects the transmission spectrum. Fig. 3c shows the resonance spectrum of the micro-ring resonator with the ISM coating. The ISM membrane has a refractive index around 1.52, resulting in slightly increased FSRs (0.61 nm). On the other hand, the increase of the refractive index in the cladding (i.e. the ISM membrane) also causes increased bending losses for small micro-rings. Optical simulations of Finite-Difference Time-Domain method using Lumerical indeed show that the optical bending loss increases from 3 dB/cm to 800 dB/cm when the coating refractive

index increases from 1.33 to 1.50 for a bending radius of 30 μm . From the magnetic field distribution (insets of Fig. 3e) of the ring cross-section, it is evident that the mode leaks out when the refractive index of the coating is very close to that of the SU8 waveguide (1.564 at 765 nm). Besides, the ISM coating introduces additional absorption losses that lead to a decreased Q factor of 10,000. The functionalized micro-ring resonators still exhibits a nearly symmetric resonance peak with a somewhat broader resonance with a linewidth of around 80 pm, as shown in Fig. 3c and d. This determines a measurable refractive index change of $\sim\!10^{-3}$.

2.3. Nitrate ion-concentration sensing

The response of a functionalized micro-ring resonator device to the presence of nitrate ions was studied by refractometry measurements. During the measurement, the laser wavelength is set to continuously sweep over a 3 nm range, started at 765 nm at constant power and the transmission spectra are recorded in real time. Initially, nitrate ionophore-cocktail A, i.e. the commercial ISM cocktail used for potentiometric sensing approaches, was used as-received to functionalize the micro-ring photonic sensor with a coating thickness of ~100 nm. Multiple resonances are observed within the measured wavelength range (Fig. 3c), and the redundancy provides additional reliability by averaging the results from different resonances. When the photonic sensor is exposed to nitrate solutions with different concentrations, the refractive index of the ISM coating changes due to the ion diffusion into the membrane from the aqueous phase, which in turn results in a shift in the optical resonance wavelength of the micro-resonator. However, the sensor functionalized by the commercial ISM cocktail exhibited poor

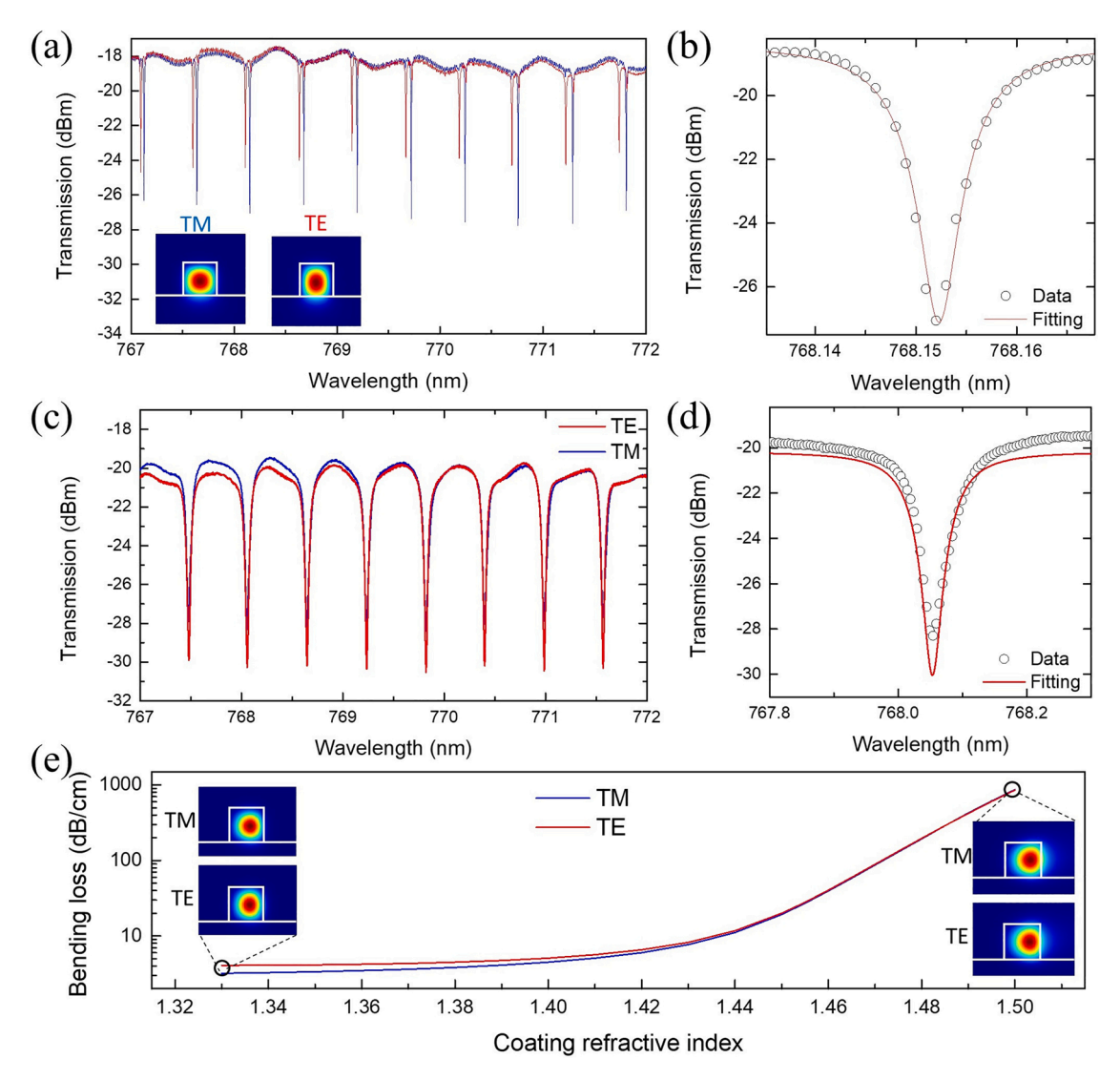
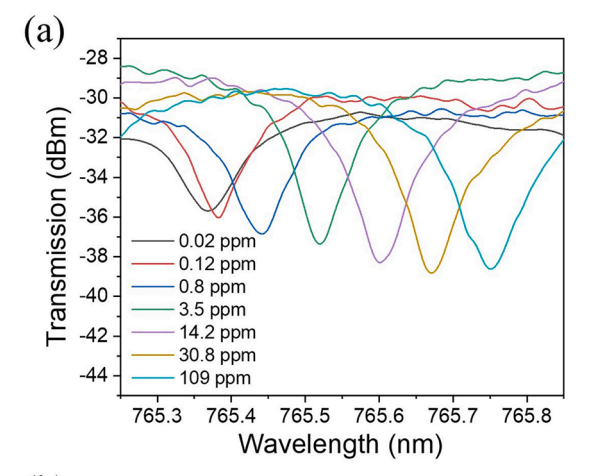


Fig. 3. (a) Experimental optical transmission spectrum of a microresonator without a functionalization coating; Inset of (a) shows the magnetic field distribution of the transverse-electric (TE) and transverse-magnetic (TM) modes; (b) Zoomed-in spectrum of one optical resonance, showing a linewidth of 8 pm; (c) Experimental optical transmission spectrum of a microresonator with a 100 nm ISM coating; (d) Zoomed-in spectrum of one optical resonance for the functionalized device; The spectra in (b) and (d) are fitted to a Lorentzian lineshape; (e) Bending loss of a $1 \times 1 \mu m^2$ SU8 waveguide (with a bending radius of 30 μ m) as a function of refractive index of the functionalization coating at 770 nm wavelength; Inset of (e) shows the magnetic field distribution of the TE and TM modes at n = 1:33 (low bending loss) and n = 1:50 (high bending loss), respectively.

sensitivity, i.e., the total resonance shift is only 0.3 Å when varying the nitrate concentration from 0.02 ppm to 109 ppm, as shown in Fig. S1.

To enhance the sensitivity, the concentration of the nitrate ionophore in the ISM membrane was increased from 1.5 wt.% to 6.2 wt.% by adding additional TDDMA to the precursor cocktail solution. A higher ionophore concentration can lead to larger changes in the refractive index of the functional coating upon changing the nitrate concentration. Further increasing the ionophore content however can lead to the ionophore precipitation during the drying process. By pipetting sodium nitrate solutions onto the photonic sensor, the nitrate concentration is continuously varied from 0.02 ppm to 109 ppm. Fig. 4 shows the refractometric measurement results as a function of solution concentration. With respect to the standard solution containing 0.02 ppm sodium nitrate, a resonance shift was clearly observed at a concentration as low as 0.1 ppm. Each test was performed under the controlled experimental condition where the optical transmission spectrum was continuously recorded within a given exposure time of 5 min. after each concentration adjustment. For each test, the resonance dip gradually shifted and always stabilized within 4 min (Fig. S2), indicating the

relatively fast response of this ISM-functionalized photonic sensor. With the nitrate concentration increasing, the optical resonances shift towards longer wavelengths, implying an increased refractive index. The optical resonances are directly correlated with the nitrate concentration. Numerical fitting gives a relationship of $S = 1.47*\log N + 0.783$, where Sis the resonance shift in a unit of Å, while N is the nitrate concentration in a unit of ppm. In this case the shift is 3 Å for a nitrate concentration change from 1 ppm to 100 ppm, significantly higher than the case of the commercial ISM precursor cocktail. This integrated photonic sensor shows an unambiguous correlation with the nitrate concentration within the relevant range of nitrate detection desirable for soil science (~few to ~100 ppm), ensuring a satisfactory detection range comparable to ISEs. Note that the microresonator-based photonic device captures resonance dips with a high resolution while providing repeatable, consistent results. As shown in Fig. S3, when the nitrate concentration is fixed, the resonance dip barely changes in position during wavelength sweeping for 10 cycles over a 4 Å range. The standard deviation of the resonance shift was calculated to be \pm 0.6 pm, and corresponds to a resolution of approximately ~1 ppm in terms of uncertainty in the nitrate



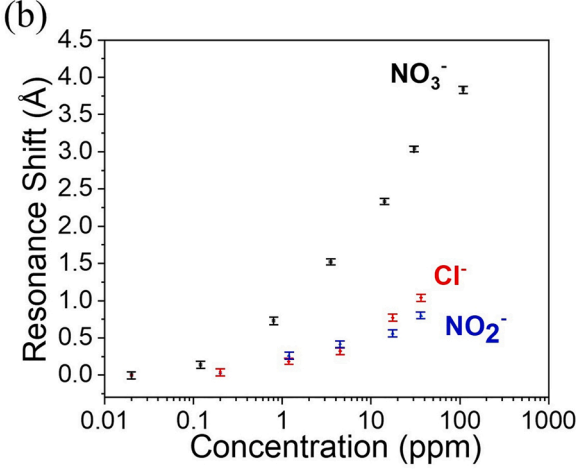


Fig. 4. (a) Optical transmission spectrum of a nitrate-ISM-functionalized in nitrate solutions with difference concentration; (b) Resonance shift as a function of ion concentration in three different solutions. Error bars are obtained based on five parallel wavelength scans.

concentration. Coupled with the high-spectral-resolution tunable laser that can resolve the sub-pm shift in the optical resonance, the nitrate concentration can be accurately determined using the integrated photonic sensor. Compared with ISEs that can suffer from degraded accuracy caused by the intrinsic potential drift from a reference electrode [31], the integrated photonic sensor shows potential advantages in terms of accuracy and stability of measurement. Note that the resolution of $\sim\!1$ ppm is obtained under laboratory settings with ultra-high precision laboratory grade equipment. Under field conditions, for in-situ sensing, we anticipate that compact optical setups based upon portable tunable lasers will be used. The resolution may be lower under such circumstances. This is the subject of further study and is outside the scope of this investigation.

The use of thicker ISM films results in a continual drift of the resonance peak position without stabilizing within 10 min of the start of the test. The results are shown in Fig. S4 in the supplemental section. This can be attributed to the slow diffusion process from the aqueous solution to the hydrophobic plasticized polymer phase. For practical use, a quick and stable response is preferred. Therefore, a thin film layer of ISM (e.g., 100 nm) is more suitable as the functionalization coating for microresonator photonic sensors.

To investigate the selectivity of such ion-selective microresonator sensors, control experiments were then carried out using sodium solutions with ${\rm Cl^-}$ and ${\rm NO_2^-}$. The ${\rm Cl^-}$ ion widely exists in agricultural soil and water at a concentration of tens to hundreds ppm, comparable with the nitrate concentration in the environment. Because of the strong

similarity between chloride and nitrate anions in terms of their hydrated radius and charge, differentiating between Cl^- and NO_3^- by common sensor techniques is always challenging. On the other hand, a nitrate sensor is required to show selectivity over nitrite ions, since for agricultural studies purposes the nitrate concentration is of importance. The measurement results of selectivity are shown in Fig. 4b. Unlike the case for the nitrate solutions, the correlation between the resonance shift and the anion concentrations of NO_2^- and Cl^- is negligible when the concentration is below 10 ppm. When exposing to a solution with a concentration above 10 ppm, the photonic sensor maintains an excellent selectivity for nitrate, where the resonance shift is four times larger than that of the other anions at the same concentration.

3. Conclusions

To summarize, we have demonstrated a chip-scale photonic sensing platform for nitrate ion sensing with high sensitivity and specificity when it is coated with a nitrate-selective ISM as a functionalizing membrane. Our study shows that the ISM serves as a low absorption loss optical coating whose refractive index changes as a function of nitrate content. These small changes are detected via shifts in the resonance peaks of the ring-microresonator structure based photonic device. The device is exposed to sodium nitrate solutions of various concentrations, and the measured resonance shift shows an unambiguous correlation with the nitrate concentration from between $1-100 \,\mathrm{ppm}$, a nitrate detection sensitivity of 0.1 ppm, and good specificity against Cl⁻ and NO₂ ions. The shifts themselves, are within the reach of compact solidstate lasers (such as distributed feedback lasers) and detectors so that this approach may be suitable for compact field deployable units using integrated photonic technologies. Using the functionalized membranes, our experiments also demonstrate a new approach for utilizing ISMs for sensing applications, providing new opportunities in sensing for not only nitrate ions but a wide range of ions where ISMs are available.

CRediT authorship contribution statement

Zhongbo Zhang: Methodology, Investigation, Validation, Data curation, Writing - original draft. Xufeng Zhang: Conceptualization, Methodology, Writing - review & editing. Tijana Rajh: Methodology. Supratik Guha: Conceptualization, Writing - review & editing.

Declaration of Competing Interest

The authors reported no declarations of interest.

Acknowledgements

This research was funded by the National Science Foundation (Award No. 1841652). This work was performed at the Center for Nanoscale Materials, Argonne National Laboratory. Use of the Center for Nanoscale Materials, an Office of Science user facility, was supported by the U.S. Department of Energy, Office of Science, Office of Basic Energy Sciences, under Contract No. DE-AC02-06CH11357. The authors thank Dr. Ralu Divan, Dr. David Czaplewski, and Dr. Leonidas Ocola for helping in device fabrication, and Dr. Houcheng Chang for helping with the functionalization coating.

Appendix A. Supplementary data

Supplementary material related to this article can be found, in the online version, at doi:https://doi.org/10.1016/j.snb.2020.129027.

References

[1] H. Di, K. Cameron, How does the application of different nitrification inhibitors affect nitrous oxide emissions and nitrate leaching from cow urine in grazed

- pastures? Soil Use Manage. 28 (2012) 54-61, https://doi.org/10.1111/j.1475-
- [2] J. Dymond, A.G. Ausseil, R. Parfitt, A. Herzig, R. McDowell, Nitrate and phosphorus leaching in new zealand: a national perspective, N. Z. J. Agric. Res. 56 (2013) 49–59, https://doi.org/10.1080/00288233.2012.747185.
- [3] V.I. Adamchuk, J.W. Hummel, M.T. Morgan, S.K. Upadhyaya, On-the-go soil sensors for precision agriculture, Comput. Electron. Agric. 44 (2004) 71–91, https://doi.org/10.1016/j.compag.2004.03.002.
- [4] D. Wegmann, H. Weiss, D. Ammann, W.E. Morf, E. Pretsch, K. Sugahara, W. Simon, Anion-selective liquid membrane electrodes based on lipophilic quaternary ammonium compounds, Microchim. Acta 84 (1984) 1–16, https://doi.org/ 10.1007/BF01204153.
- [5] A.S. Watts, V.G. Gavalas, A. Cammers, P.S. Andrada, M. Alajarin, L.G. Bachas, Nitrate-selective electrode based on a cyclic bis-thiourea ionophore, Sens. Actuators B Chem. 121 (2007) 200–207, https://doi.org/10.1016/j. snb.2006.09.048.
- [6] A. Seichi, N. Kozuka, Y. Kashima, M. Tabata, T. Goda, A. Matsumoto, N. Iwasawa, D. Citterio, Y. Miyahara, K. Suzuki, Real-time monitoring and detection of primer generation-rolling circle amplification of DNA using an ethidium ion-selective electrode, Anal. Sci. 32 (2016) 505–510, https://doi.org/10.2116/analsci.32.505.
- [7] L. Campanella, C. Colapicchioni, G. Crescentini, M. Sammartino, Y. Su, M. Tomassetti, Sensitive membrane isfets for nitrate analysis in waters, Sens. Actuators B Chem. 27 (1995) 329–335, https://doi.org/10.1016/0925-4005(94) 01612-1.
- [8] C. Jimenez-Jorquera, J. Orozco, A. Baldi, ISFET based microsensors for environmental monitoring, Sensors 10 (2010) 61–83, https://doi.org/10.3390/ s100100061.
- [9] D. Yu, Y. Wei, G. Wang, Time-dependent response characteristics of ph-sensitive ISFET, Sens. Actuators B Chem. 3 (1991) 279–285, https://doi.org/10.1016/0925-4005(91)80018-F.
- [10] M.J. Moorcroft, J. Davis, R.G. Compton, Detection and determination of nitrate and nitrite: a review, Talanta 54 (2001) 785–803, https://doi.org/10.1016/S0039-9140(01)00323-X
- [11] H.W. Jannasch, K.S. Johnson, C.M. Sakamoto, Submersible, osmotically pumped analyzer for continuous determination of nitrate in situ, Anal. Chem. 66 (1994) 3352–3361, https://doi.org/10.1021/ac00092a011.
- [12] M. Huebsch, F. Grimmeisen, M. Zemann, O. Fenton, K. Richards, P. Jordan, A. Sawarieh, P. Blum, N. Goldscheider, Technical notes: field experience using uv/ vis sensors for high-resolution monitoring of nitrate in ground water, Hydrol. Earth Syst. Sci. 19 (2015) 1589–1598, https://doi.org/10.5445/IR/1000046934.
- [13] M. Hidaka, A. Gotoh, T. Shimizu, K. Minamisawa, H. Imamura, T. Uchida, Visualization of NO₃/NO₂ dynamics in living cells by fluorescence resonance energy transfer (FRET) imaging employing a rhizo-5 bial two-component regulatory system, J. Biol. Chem. 29 (2016) 2260–2269, https://dx.doi.org/ 10.1074%2Fibc.M115.687632.
- [14] A. Buldt, U. Karst, Determination of nitrite in waters by microplate fluorescence spectroscopy and HPLC with fluorescence detection, Anal. Chem. 71 (1999) 3003–3007, https://doi.org/10.1021/ac981330t.
- [15] M. Yaqoob, B. Biot, A. Nabi, P. Worsfold, Detection of nitrate and nitrite in freshwaters using flow-injection with luminol chemiluminescence detection, Luminescence 27 (2012) 419–425, https://doi.org/10.1002/bio.1366.
- [16] A. Shaviv, A. Kenny, I. Shmulevitch, L. Singher, Y. Raichlin, A. Katzir, Direct Monitoring of soil and water nitrate by FTIR based FEWS or membrane systems, Environ. Sci. Technol. 37 (2003) 2807–2812, https://doi.org/10.1021/es020885
- [17] M. Trivedi, A. Branton, D. Trivedi, G. Nayak, K. Bairwa, S. Jana, Spectroscopic characterization of disodium hydrogen orthophosphate and sodium nitrate after biofield treatment, Chromatogr. Sep. Tech. 6 (2015) 1000282, https://doi.org/ 10.4172/2157-7064.1000282.
- [18] A. Ianoul, T. Coleman, S. Asher, UV resonance raman spectroscopic detection of nitrate and nitrite in wastewater treatment processes, Anal. Chem. 74 (2002) 1458–1461, https://doi.org/10.1021/ac010863q.
- [19] N.A. Yebo, P. Lommens, Z. Hens, R. Baets, An integrated optic ethanol vapor sensor based on a silicon-insulator microring resonator coated with a porous ZnO film, Opt. Express 18 (2010) 11859–11866, https://doi.org/10.1364/OE.18.011859.

- [20] K. Xu, Y. Chen, T.A. Okhai, L.W. Snyman, Micro optical sensors based on avalanching silicon light-emitting devices monolithically integrated on chips, Opt. Mater. Express 10 (2019) 3985–3997, https://doi.org/10.1364/OME.9.003985.
- [21] S. Wakida, M. Yamane, A. Kawahara, S. Takasuka, K. Higashi, Durable poly(vinyl chloride) matrix ion-selective field effect transistors for nitrate ions, Bunseki Kagaku 38 (1989) 510–514, https://doi.org/10.2116/bunsekikagaku.38.10_510.
- [22] M. Knoll, K. Cammann, C. Dumschat, C. Sundermeier, J. Eshold, Potentiometric silicon microsensor for nitrate and ammonium, Sens. Actuators B Chem. 18 (1994) 51–55, https://doi.org/10.1016/0925-4005(94)87055-1.
- [23] M. Gartia, B. Brauschweig, T.W. Chang, P. Moinzadeh, B. Minsker, G. Agha, A. Wieckowski, L. Keefer, G. Liu, The microelectronic wireless nitrate sensor network for environmental water monitoring, J. Environ. Monit. 14 (2012) 3068, https://doi.org/10.1039/c2em30380a.
- [24] J. Artigas, C. Jimenez, S.G. Lemos, A. Nogueira, A. Torre-Neto, J. Alonso, Development of a screen-printed thick-film nitrate sensor based on a graphiteepoxy composite for agricultural applications, Sens. Actuators B Chem. 88 (2003) 337–344, https://doi.org/10.1016/S0925-4005(02)00399-4.
- [25] D. Freiner, R. Kunz, D. Citterio, U. Spichiger, M. Gale, Integrated optical sensors based on refractometry of ion-selective membranes, Sens. Actuators B Chem. 29 (1995) 277–285, https://doi.org/10.1016/0925-4005(95)01694-5.
- [26] X. Xie, M. Pawlak, M. Tercier-Waeber, E. Bakker, Direct optical carbon dioxide sensing based on a polymeric film doped with a selective molecular tweezer-type ionophore, Anal. Chem. 84 (2012) 3163–3169, https://doi.org/10.1021/ ac2030046
- [27] G. Kim, K. Sudduth, S. Grant, N. Kitchen, Disposable nitrate-selective optical sensors based on fluorescent dye, J. Biosyst. Eng. 37 (2012) 209–213, https://doi. org/10.5307/JBE.2012.37.3.209.
- [28] M. Knoll, K. Cammann, C. Dumschat, C. Sundermeier, J. Eshold, Potentiometric silicon microsensor for nitrate and ammonium, Sens. Actuators B Chem. 18 (1994) 51–55, https://doi.org/10.1016/0925-4005(94)87055-1.
- [29] M. Knoll, K. Cammann, C. Dumschat, J. Eshold, C. Sundermeier, Micromachined ion-selective electrodes with polymer matrix membranes, Sens. Actuators B Chem. 21 (1994) 71–76, https://doi.org/10.1016/0925-4005(94)01227-X.
- [30] K. Xu, Monolithically integrated Si gate-controlled light-emitting device: science and properties, J. Opt. 20 (2018) 024014, https://doi.org/10.1088/2040-8986/ aaa2b7.
- [31] B.A. Pellerin, B.A. Bergamaschi, B.D. Downing, J.F. Saraceno, J.D. Garrett, L. D. Olsen, Optical techniques for the determination of nitrate in environmental waters: guidelines for instrument selection, operation, deployment, maintenance, quality assurance, and data reporting. Collection of Water Data by Direct Measurement, Geological Survey, 2013, pp. 1–37, https://doi.org/10.3133/tm1D5.

Zhongbo Zhang completed his Ph.D. with Case Western Reserve University, US (2018). He is currently a postdoctoral scholar at the University of Chicago. His research interests include functional polymers and their applications in electrical, electronic, and photonic devices, currently focusing on the development of an integrated photonic sensing platform for soil sensing applications.

Xufeng Zhang is an assistant scientist at Center for Nanoscale Materials, Argonne National Laboratory (US). He received his Ph.D. degree in Electrical Engineering from Yale University in 2016. His research interests focus on spin wave device physics and environmental sensor/sensor networks.

Tijana Rajh is a senior materials scientist at Argonne National Laboratory (US). Her research focuses on surface modification of nanocrystalline ${\rm TiO_2}$ nanoparticles for light-induced metal sequestration, deposition of metallic nanocircuits, and integration with biomolecules.

Supratik Guha is a professor in the Pritzker School for Molecular Engineering at the University of Chicago (US), and is also a senior advisor to the Physical Sciences and Engineering directorate at Argonne National Laboratory. He received his Ph.D. in materials science in 1991 from the University of Southern California. His research interests are focused on new materials, devices, and systems for information processing and quantum technology.